

# UNDERSTANDING AND CONTROL OF UNSTABLE CONTACT RESISTANCE IN RF MEMS GOLD-GOLD DIRECT CONTACT SWITCHES

Linda L.W. Chow\* and Katsuo Kurabayashi  
University of Michigan, Ann Arbor, USA

\*Currently with Intel Corporation, Chandler, U.S.A. Email: Linda.l.chow@intel.com

## ABSTRACT

The implementation of direct contact RF MEMS switches is challenging owing to their unstable contact resistance and low power handling/delivery. This paper carefully studies RF MEMS switch contact behavior and proposes a new method to suppress its instability leading to device failure. Our study supports the hypothesis that MEMS contact switches fail primarily due to contact necking. Using the proposed method, we demonstrate the ability to keep MEMS switch contact resistance under  $\sim 0.05 \Omega$  in high-cycle cold-switching while a high contact current of  $>0.9 \text{ A}$  is handled/delivered.

## INTRODUCTION

Direct contact radio frequency microelectromechanical systems (RF MEMS) switches have been envisioned as ideal building blocks for Radio-On-Chip development [1], due to its ultra wide-band (DC to 100 GHz), ultra-low insertion loss ( $< 0.1 \text{ dB}$ ), high isolation ( $< -40 \text{ dB}$ ), and high linearity [2]. The contact material is mostly pure gold-gold for low ultra-loss consideration and ease/low-cost of fabrication compared to the highly precise control of dopants. However, in commercialization, there are two critical reliability challenges: unstable contact resistance,  $R_C$ , and low power handling/delivery.

Extensive research has been performed to study the contact behavior of the switches during cyclic switching for various parameters such as contact force [3-4], contact materials [5-6], apparent contact area [7], contact current [8], and contact voltage,  $V_C$ , [9-10]. Nevertheless, the mechanisms governing the unstable  $R_C$  still remains unclear. As plotted in Fig. 1,  $R_C$  generally rises at  $V_C$  lower than the softening voltage,  $V_{Softening}$ , at which a sudden drop of the contact resistance occurs. And as in Fig 2, the  $R_C$  drops when the  $V_C$  is higher than the  $V_{Softening}$  due to contact softening [10].

In this paper, we systematically study the contact mechanisms driving the  $R_C$  increase, and propose self-healing control circuitry to achieve stable  $R_C$  even in high power handling/delivery.

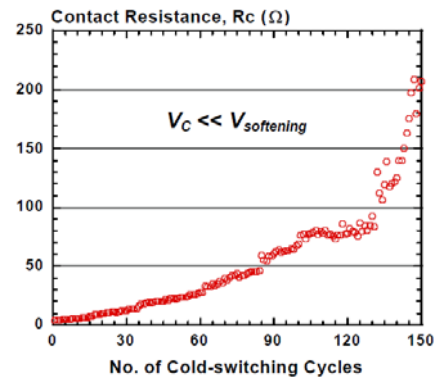


Figure 1: Typical unstable contact resistance response: increasing at low ( $\sim 10 \text{ mV}$ ) contact voltage.

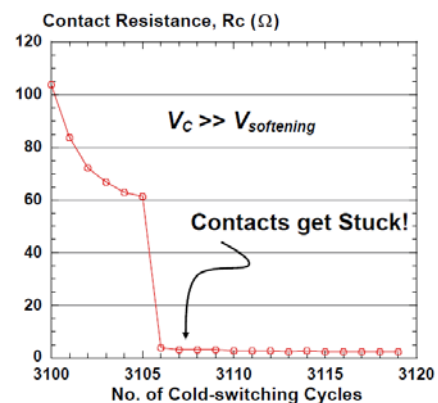


Figure 2: Typical unstable contact resistance response: reducing at high ( $\sim 200 \text{ mV}$ ) contact voltages. And contacts eventually get stuck.

## HYPOTHESES

We first propose 3 hypotheses to account for the switch failure mechanism: Hypothesis A (Fig. 3) suggests that contact asperities elongate and undergo mechanical necking during switch cycling. Hypothesis B (Fig. 4) proposes that they encounter surface hardening with dislocations built-up from mechanical cold work. And hypothesis C (Fig. 5) advocates that the contaminant film (C-film) gets thickened as hydrocarbons accumulate from the atmosphere on the increasing defect sites and reduces the contact asperity area/radius.

## EXPERIMENTAL SETUP

We designed and fabricated RF MEMS pure gold-gold direct contact switches with the conventional fabrication process [11], and then characterized the  $R_C$  by 4-wire I-V measurement in a vacuum chamber of 1-2 mTorr. The minimal actuation voltage of 55 V was recorded by slowly increasing the power supply voltage from zero until the contacts first became conductive. Using the pure Euler-Bermoulli beam bending analysis, the contact force is estimated to be very small ( $<20$  uN).

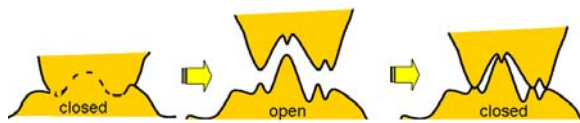


Figure 3: Hypothesis-A: Contact asperities elongate then neck during the switch opening.

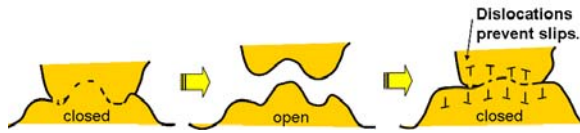


Figure 4: Hypothesis-B: Contact asperities encounter surface hardening with dislocation built-up as experienced mechanical (cold) work.

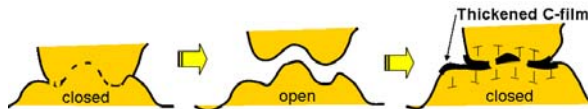


Figure 5: Hypothesis-C: Contaminant film (C-film) gets thickened owing to the preferred adsorption of contaminants on surface defects such as the increasing hardening-induced dislocations.

## EXPERIMENTS & RESULTS

First, we intentionally increased the contact force by actuation voltage while keeping the  $V_C$  lower than the  $V_{Softening}$ , corresponding to  $R_C$  and its accompanying contact asperity radius [10, 12] (Fig. 6) as to avoid contact softening. As shown in Fig. 7,  $R_C$  drops with the contact force. Thus, contact hardening is unlikely the dominant mechanism, which eliminates Hypothesis-B.

Then, we increased the  $V_C$  while keeping contact force constant as in Fig. 8. The C-film can be estimated to be nanometer thick. The very high electric field of 1G V/m, brought by  $V_C = 1V$ , should break down the C-film, and does not accumulate more hydrocarbons to shrink the contact asperity area/radius.

The resulting increase of  $R_C$  disproves Hypothesis-C. As such, only the hypothesis A is the most plausible.

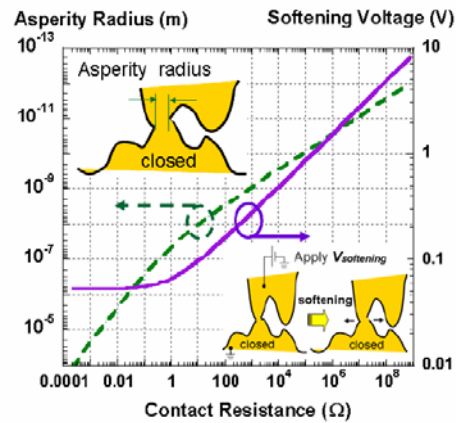


Figure 6: Plots of pure gold contact asperity radius and softening voltage required versus corresponding contact resistance [10, 12].

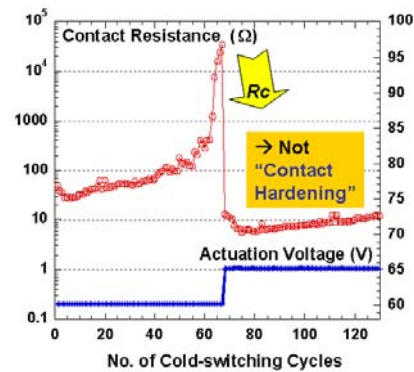


Figure 7: Contact force increase by actuation voltage resulting in  $R_C$  reduction eliminates Hypothesis-B.

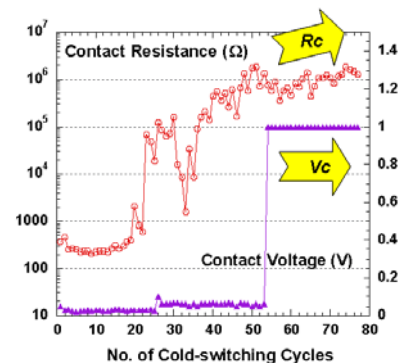


Figure 8: A  $V_C$  of 1V should break down the C-film, but the continuously increasing  $R_C$  disproves Hypothesis-C.

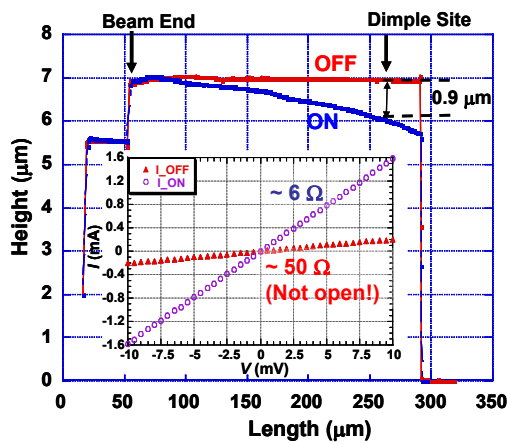


Figure 9: Real-time switch deflection and 2-wire I-V measurements at switch-on and off by interferometer showing ohmic behavior at off-state implies a metallic connection between the switch dimples and substrate pad.

### FURTHER VALIDATION

To further validate the Hypothesis-A, we set up a real-time switch deflection and resistance experiment using an interferometer simultaneously with a 2-wire I-V measurement.

In the inset figure of Fig. 9, a non-zero off-current with an increasing voltage across the contacts shows an ohmic contact behavior when the switch deflects back up. This implies that there is a metallic connection bridging the contacts upon switch-off.

We took switches after  $\sim 1$  million cycles of switching and carefully flipped over the contact dimples, we found multiple nanoscale wires protruded from the contact dimples (Fig. 10).

To verify that these nanoscale protrusions are gold wires, and not carbon-based residuals after the photoresist sacrificial layer removal in fabrication, an elemental line mapping on the switch dimple surface across line A-B (in the inset figure of Fig. 11) was conducted using Energy-dispersive X-ray spectroscopy (EDX). The EDX count shows the wire is made of gold. Therefore, this confirms our postulation (Hypothesis-A) that asperity elongation and necking cause  $R_C$  to increase.

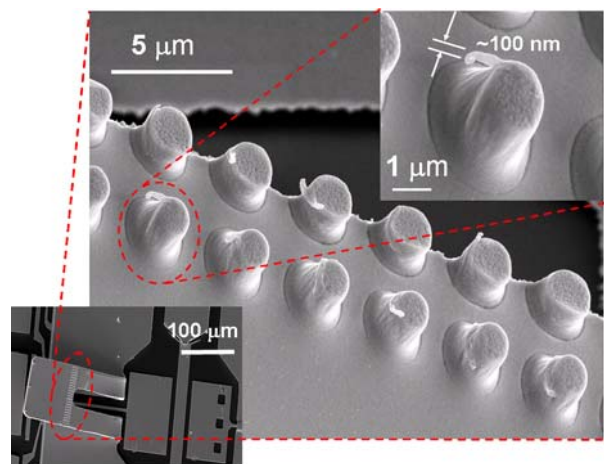


Figure 10: SEM images of multiple nanoscale wires protruded from the contact dimple of a flipped switch after  $\sim 1$  million cycles of switching.

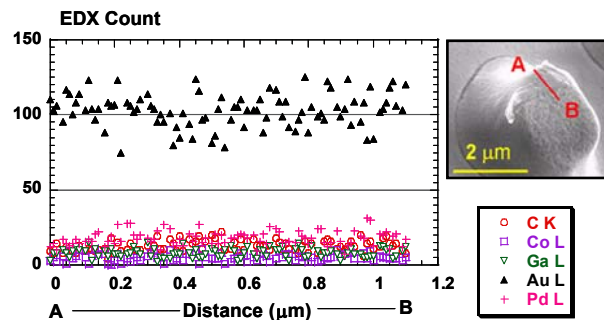


Figure 11: EDX line mapping of nanoscale wire elongated from the switch contact dimple (across A-B in the inset figure) proves the wire is made of gold.

### STABLE CONTACT RESISTANCE & HIGH POWER HANDLING/DELIVERY

With the knowledge obtained above, we designed a new simple self-healing feedback control circuitry to achieve long-term stability of  $R_C$  with high power handling/delivery: adding a constant resistance,  $R_0$ , in series with the switch (as in Fig. 12).  $V_C$  can then be controlled in the simple electrical potential divider circuitry. The addition of  $R_0$  can be easily implemented by adding a resistive transmission line on a high speed/frequency printed circuit board, or by connecting an add-on on-shelf resistor in series.

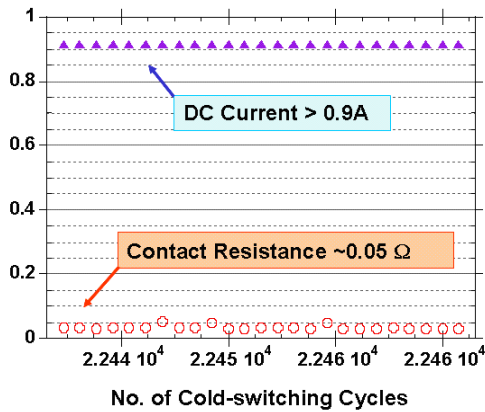


Figure 13: Real-time switch deflection and 2-wire I-V measurements at switch-on and off by interferometer showing ohmic behavior at off-state implies a metallic connection between the switch dimples and substrate pad.

The basic operation principle is as follows: During cyclic switching at low  $V_C$ ,  $R_C$  increases. When  $R_C$  is getting much larger than  $R_0$ ,  $V_C$  approaches  $V_{Softening}$ , and  $R_C$  will drop drastically. Nonetheless, when  $R_C$  drops to much smaller than  $R_0$ ,  $V_C$  drops to zero and softening stops.

We connected this control circuitry to our switches and performed cold-switching. As Fig. 13 plotted, it has successfully demonstrated that the contact resistance can be maintained at  $\sim 0.05 \Omega$  in high-cycle cold-switching while a high contact current of  $>0.9 \text{ A}$  can be handled/delivered. There is no high contact resistance spikes recorded. And the switches have not become stuck. In a transmission line of  $50 \Omega$  characteristic impedance, this corresponds to high RF power handling/delivery of  $>40 \text{ W}$ .

## CONCLUSIONS

In this paper, three hypotheses were postulated as the root cause of RF MEMS contact switch failure: (A) contact necking, (B) hardening, and (C) contamination film thickening. After careful characterizations using resistance/switch deflection measurement, SEM imaging and EDX elemental mapping, hypothesis (A) was fully validated. To control the unstable contact resistance, a new self-healing feedback control circuitry was proposed, and successfully demonstrated a contact resistance under  $\sim 0.05 \Omega$  in high-cycle cold-switching with high contact current of  $>0.9 \text{ A}$ , which corresponds to high RF power handling/delivery of  $>40 \text{ W}$ .

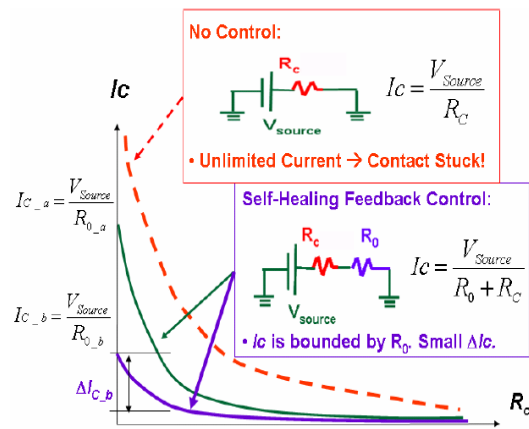


Figure 12: Using self-healing feedback control circuitry, contact current becomes bounded, and gives a stable contact resistance in switching.

## REFERENCES

- [1] P. Gammel, G. Fisher, and J. Bouchaud, "RF. MEMS and NEMS Technology, Devices, and Applications", *Bell Labs Technical Journal*, vol. 10(3), pp. 29-59, 2005
- [2] G. M. Rebeiz, *RF MEMS Theory, Design, and Technology*, New Jersey: Wiley, 2003
- [3] D. Hyman and M. Mehregany, "Contact physics of gold microcontacts for MEMS switches", *IEEE Trans. Comp. Packag. Technol.*, vol. 22(3), pp. 357-364, 1999
- [4] S. Majumdar, N. E. McGruer, G. G. Adams, P. M. Zavracky, R. H. Morrison, and J. Krim, "Study of contacts in an electrostatically actuated microswitch", *Sensors & Actuators A*, vol. 93, pp. 19-26, 2001
- [5] J. Schimkat, "Contact materials for microrelays", *11th IEEE Int. Conf. on Microelectromech. Syst.*, 1998, pp. 190-194
- [6] R. A. Jr. Coutu, P. E. Kladitis, K. D. Leedy, and R. L. Crane, "Selecting Metal Alloy Electric Contact Materials for MEMS Switches", *J. Micromechanics and Microengineering*, vol. 14(8), pp. 1157-1164, 2004
- [7] S. C. Bromley and B. J. Nelson, "Performance of microcontacts tested with a novel MEMS device", *Proc. 47th IEEE Holm Conf. Electrical Contacts*, 2001, pp. 122-127
- [8] J. DeNatale, "Reconfigurable RF circuits based on integrated MEMS switches," *IEEE Int. Solid-State Circuits Conf.*, 2004, pp. 310-311
- [9] R. Holm, *Electric Contacts – Theory and Applications*, Berlin: Springer-Verlag, 1967
- [10] B. D. Jensen, L. L. W. Chow, K. Huang, K. Saitou, J. L. Volakis, and K. Kurabayashi, "Effect of Nanoscale Heating on Electrical Transport in RF MEMS Switch Contacts", *J. Microelectromech. Syst.*, 14(5), pp. 935-946, 2005
- [11] L.L.W. Chow, J.L. Volakis, K. Saitou, and K. Kurabayashi, "Lifetime Extension of RF MEMS Direct Contact Switches in Hot Switching Operations by Ball Grid Array Dimple Design," *IEEE Electron Device Lett.*, vol. 28(6), pp. 479-481, 2007
- [12] G. Wexler, "The size effect and the non-local Boltzmann transport equation in orifice and disk geometry", *Proc. Phys. Soc.*, vol. 89, pp. 917-924, 1996